Calibration and improvement of the detection system CORTO

A. Natochii, V. Puill, L. Burmistrov, V. Chaumat, D. Breton, F. Campos, C. Cheikali, J. Maalmi, A. Stocchi, C. Sylvia, et al.

LAL/RT 15-04
January 2015

Laboratoire de l'Accélérateur Linéaire

Calibration and improvement of the detection system CORTO

Andrii Natochii[1], Veronique Puill[2], Leonid Burmistrov[2], V. Chaumat[2], D. Breton[2], F. Campos[2], C. Cheikali[2], J. Maalmi[2], A. Stocchi[2], C. Sylvia[2], J.F. Vagnucci[2], E. Bals[3], B. Genolini[4], X. Grave[4], J. Peyre[4], Mimae Kim[5], D.W. Kim[5]

[1] *Taras Shevchenko National University of Kyiv (Ukraine)*
[2] *LAL, CNRS/IN2P3, Université Paris Sud, Orsay, France*
[3] *Imperial College London (United Kingdom)*
[4] *Institut de Physique Nucléaire (IPN) d'Orsay (France)*
[5] *Gangneug-Wonju National University (GWNU) at Seoul (Republic of Korea)*

U.M.R
de
l'Université Paris-Sud

Institut National de
Physique Nucléaire et de
Physique des Particules du CNRS

LAL ~ Bât. 200 ~ B.P. 34 ~ 91898 Orsay Cedex ~ France

Calibration and improvement of the detection system CORTO

Andrii Natochii[1], Veronique Puill[2], Leonid Burmistrov[2], V. Chaumat[2], D. Breton[2], F. Campos[2], C. Cheikali[2], J. Maalmi[2], A. Stocchi[2], C. Sylvia[2], J.F. Vagnucci[2], E. Bals[3], B. Genolini[4], X. Grave[4], J. Peyre[4], Mimae Kim[5], D.W. Kim[5]

[1] *Taras Shevchenko National University of Kyiv (Ukraine)*

[2] *Laboratoire de l'Accélérateur Linéaire (LAL) d'Orsay (France)*

[3] *Imperial College London (United Kingdom)*

[4] *Institut de Physique Nucléaire (IPN) d'Orsay (France)*

[5] *Gangneug-Wonju National University (GWNU) at Seoul (Republic of Korea)*

Abstract

In Nuclear Physics and High Energy Physics the calibration and debugging of new detector systems in the early stages is possible using cosmic rays (muons). CORTO, the COsmic Ray Telescope at Orsay, located at the Linear Accelerator Laboratory (LAL) in Orsay (France), detects and reconstructs the position, time and direction of cosmic muons. We can study response of the investigated detectors with using coincidences between CORTO and this detector system. This work is devoted to the measurement of the major parameters of the facility: the X (1.8 cm) coordinate resolution and the Y (2.1 cm) resolution, given by the time resolution for the muon track (250 ps). The paper presents the basic principles of the track reconstruction, the electronics delays investigation and displays the results of running.

Keywords: *cosmic muons, track reconstruction, the detection efficiency, USB WaveCatcher, signal processing, MRPC.*

1 Introduction

1.1 Particle sources for detector test

In High-Energy Physics (HEP) and Nuclear Physics where sophisticated detector system consisting in different types of detectors with hundreds of millions readout channels (for example in the ATLAS (CERN) detector), the calibration and configuration the of subsystems can be performed with:

1. Radioactive sources $(\alpha, \beta, \gamma, n)$;
2. Lasers (γ);
3. Particle accelerators $(e^+, e^-, \mu, p, \bar{p}, d, \pi^0, \pi^+, \pi^-, K^0, K^-, K^+)$;
4. Nuclear reactors (n);
5. Neutron generators (n);

6. Cosmic rays (μ);

The use of natural radioactive sources for calibrating is quite easy and convenient, but their limited energy maximum does not allow to fully explore the detectors in HEP (for example, detectors that have very thick protective layer or significant size of insensitive zone). For improvement and calibration of photomultiplier tube one can use lasers, LEDs and different types of filament lamp. The most common way to test the detectors in real condition of running is to use particles from accelerators. However, there are several factors that complicate the use of accelerators: the limited time for each test, the fact that such complex devices are not in every laboratory, and that the test requires a large financial expense. Nuclear reactors are an alternative for obtaining neutrons which result from fission of nuclear fuel, but the use of this type of sources cannot be afforded by every laboratory. Cosmic radiation is safe and easy to use. The main component of cosmic radiation at the earth's surface consists of muons with an average kinetic energy of about 1 GeV. Although their flux does not exceed few particles on 100 cm^2 per second, the use of this type of radiation is unlimited in time and does not require a large amount of equipment. CORTO was designed and build at LAL to provide muon track reconstruction with a good accuracy. This work is dedicated to the study of properties of the instrument and its performances.

1.2 Cosmic rays

Most muons observed at the surface of the Earth are produced by primary cosmic rays in the upper atmosphere (Fig.1). They are the most numerous energetic particles arriving at sea level (Fig.2), with a flux of about 1 muon per square centimetre per second. Their mean energy is about 4 GeV. Muons, being charged particles, they interact with matter by ionizing it. The loss of energy of muons passing through the atmosphere is proportional to the amount of matter they traverse. The medium is usually characterized by its density (g/cm^3) times the distance travelled in centimetres. It's called the "interaction length" and measured in g/cm^2. The energy loss for muons is about 2 MeV per g/cm^2. The interaction depth of the atmosphere is about 1000 cm^2, so muons lose about 2 GeV in passing through it.

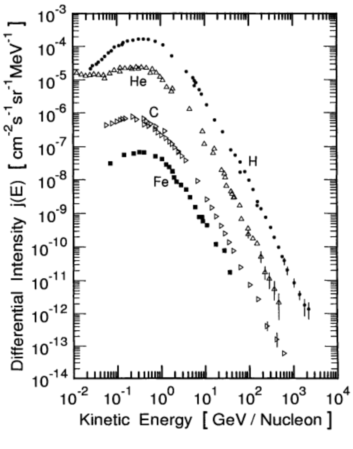

Figure 1: The main components of primary cosmic rays in the upper atmosphere; differential flux as a function of kinetic energy.[1]

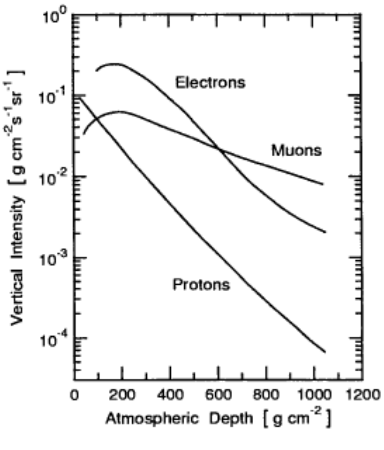

Figure 2: Altitude variation of the main cosmic ray components.[1]

2 CORTO

The Cosmic Ray Telescope was developed as a platform for testing different detector devices. It gives the numbers of μ passing through the detector under test and their tracks. This telescope is assembled and in test mode for the setting. The project involves: the Laboratoire d'Accélérateur Linéaire (LAL), The Institute de Physique Nucléaire (IPN) (Orsay, France); the group GWNU(Korea, at Gangneung-Wonju National University) and Taras Shevchenko National University of Kyiv(Ukraine).

2.1 Structure

CORTO consists of two positional sensitive strip gas detectors, called Multigap Resistive Plate Chamber (MRPC)(1 m $\times$ 2 m $\times$ 5 cm), which provide the track reconstruction. These detectors are spaced vertically at a distance of 2 m (see Fig.3). Between them are placed moving platforms for accommodating the research detection devices. Electronics for CORTO is situated on a separate platform for convenience. A controlled system assures the gas supply for MRPC.

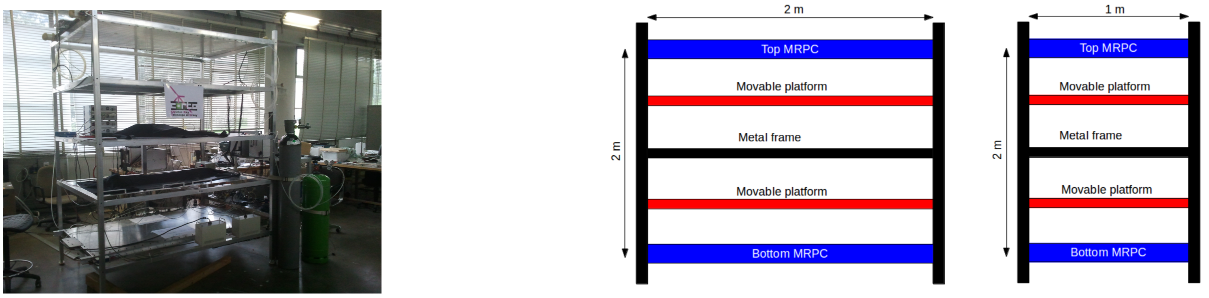

Figure 3: CORTO: picture (left) and drawing (right).

2.2 Multigap Resistive Plate Chamber

2.2.1 Structure

The MPRCs[2] used for CORTO were originally produced for the ALICE Experiment at CERN, having then been adapted for the Extreme Energy Events (EEE) project. They are composed of a total of seven glass plates, being separated by six gas gaps each of 300 μm width. Their readout electrode is segmented with 24 strips (2.5 cm $\times$2 m). The complete MRPC unit is housed within an outer, gas-tight, aluminium casing with inputs for the electronics, voltage supply, and gas entry and exit.

2.2.2 Gas Mixture

The standard gas mixture used in modern RPCs and MRPCs primarily contains tetrafluoroethane ($C_2H_2F_4$, Freon 134-a, provides a "heavy" electronegative gas), a small proportion of SF_6, and, occasionally, a small proportion of iso-butane C_4H_{10}. MRPCs are operated at LAL with pure $C_2H_2F_4$.

2.2.3 Readout of the strips

There are 24 differential outputs (from left and right sides) at each MRPC. Multiple gas gaps within the MRPC mean that multiple avalanches are created for a single incident muon traversing the chamber. The inner plates act as dielectrics and so are transparent to the fast signals produced by the electron avalanche. The induced signals on the pickup strips are therefore due to the sum of the signals from the avalanches in all of the gas gaps. Knowing the length of each strip and the speed of the signals, the hit position can be retrieved from a measurement of the difference in signal time arrival.

2.3 Electronics

The signal collected on the strips is sent to a front-end electronic circuit based on ultra-fast channel amplifier/discriminator cards based on NINO-ASIC chips. The amplified signals are transferred by the interface card to the WaveCatcher, high-performance digitizing boards based on a new generation of ultra fast analog memories[3].
The NINO Application-Specific Integrated Circuit (ASIC)[4] was developed as an amplifier explicitly for the differential input of the MRPC. NINO generates a Low Voltage Differential Signal (LVDS) output with a width dependent logarithmically on the input charge. Its previous amplifier provides good resolution in time (jitter) of less than 25 ps[5].
The interface card serves to convert the signals of the NINO from differential to monopolar (common mode) form, this being required as an input of the WaveCatcher boards. The interface board also serves to split the input from the 68 SCSI cable into 24 individual cables, allowing signals from each pickup strip (anode-cathode pairing) to be sent via an individual cable to the WaveCatcher boards. The signals are then sent via USB input, to the computer and the custom-built software.
The WaveCatcher has a time resolution of $\sim$ 7 ps. The size of analog memory is 1024 points, so when the distance between adjacent digitized points is 312.5 ps the total memory depth is 320 ns.
Each WaveCatcher board has a total of 16 input channels and so, for all the strips' cables to be connected, 6 WaveCatcher boards will be required in the final set-up for the total readout of the 96 signals.
The software for the WaveCatcher provides an oscilloscope-like display, allow that to analyze the signals and to save the information to a computer.

2.4 Reconstruction of the X and Y coordinates

Cosmic rays passing through the MRPC induce signals on the strip, which is then readout by the electronics. The coordinates in the plane of the MRPC are defined in Fig.5. The Y coordinates corresponds to the number of the strip from which the signal has come. Knowing the length of the strip (L) and the speed of signal propagation (v) on it, we can reconstruct the X coordinates. Ideally, the passage of a single muon in one MRPC induces a signal only on one strip. Since the electrical signal spreads from the place of interaction in different directions, to determine the coordinates of X we need to know the time of arrival of the signal to the left edge strip (t_L) and to its right (t_R). Then by measuring the difference between these times($\triangle\, t$)(Eq.1):

$$\triangle\, t = t_L - t_R \tag{1}$$

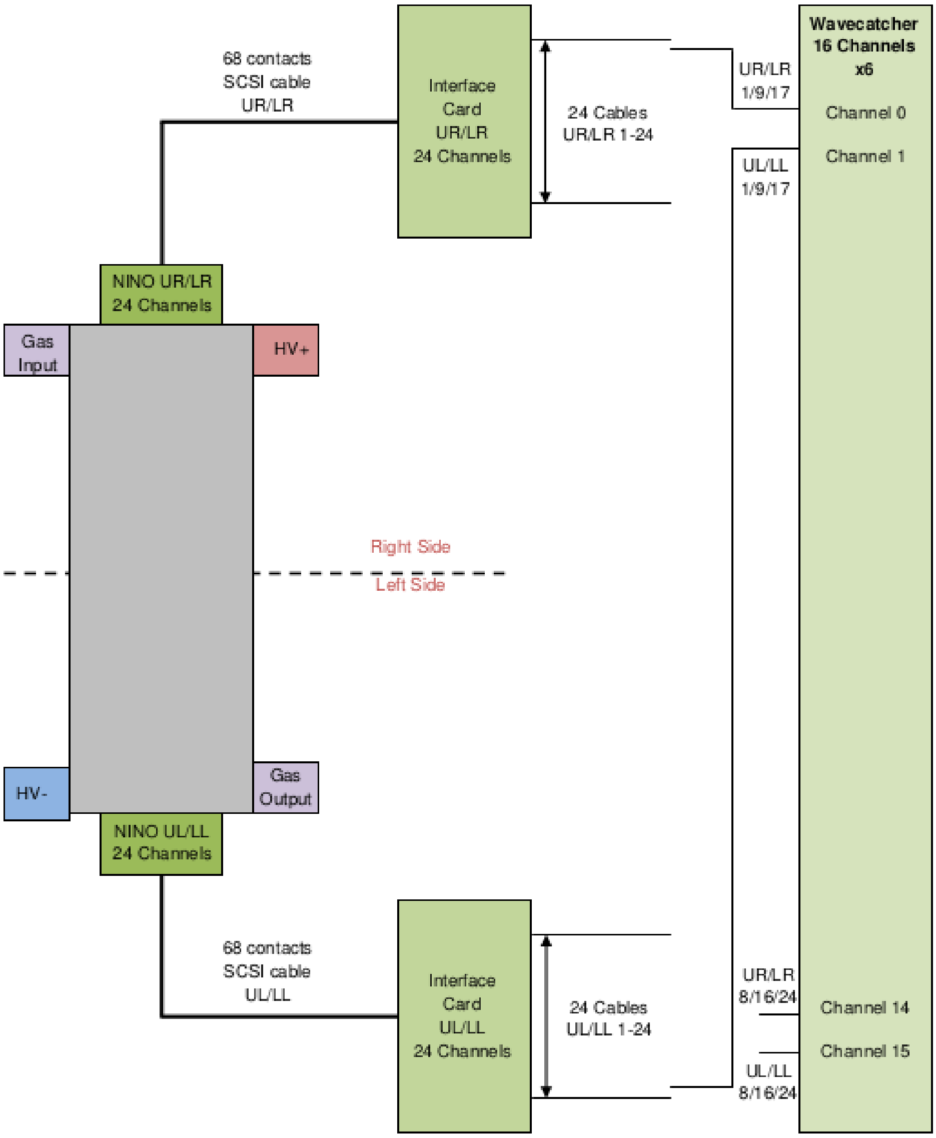

Figure 4: Schematic structure of the readout electronics. (by Chaumat Vincent)

it is possible to reconstruct the coordinates x, as follows:

$$\triangle\, t = 2 \cdot k \cdot X + T_0 \text{ ,where } k = \frac{1}{v} \tag{2}$$

T_0 is the time delay on the strip (each strip has its own).

$$X = \frac{\triangle\, t - T_0}{2 \cdot k} \equiv \frac{1}{2} \cdot (\triangle\, t - T_0) \cdot v \tag{3}$$

3 Calibration

3.1 The Electronics

The main task of the reconstruction of events is the calculation of the coordinates of the μ point of interaction in the MRPC with minimal errors. Since the signal after interaction goes a long way through

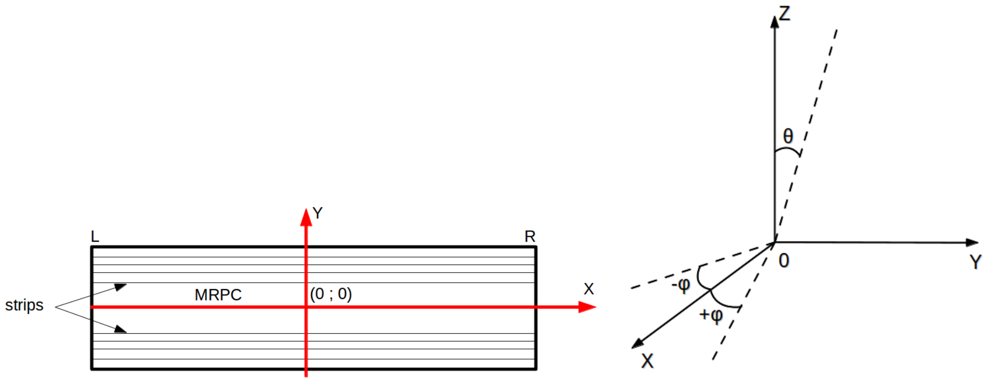

Figure 5: The coordinate system for finding the place of the muon penetration.

the electronic chain, different components of it have to be measured: the time delays associated with the NINO card (T_{NINO}), the 68 scsi cable (T_{Cable}), the interface card and the cables to the WaveCatcher (T_{Link}), and the delay added by the channel of the WaveCatcher itself ($T_{Channel}$).

3.1.1 Calibration of the WaveCatcher channels

The calibration of the WaveCatcher has to be performed with the same type of signal that is sent to the NINO chip, therefore the signal has a rectangle shape. Based on the analysis of the MRPC output signal, it was found that the width of the signal is 14 nanoseconds, with an amplitude of 300 mV. Therefore, these parameters were chosen for the signal generator which was used to calibrate the WaveCatcher boards (Fig.6). The correction of the WaveCatcher delay can then be done by subtracting the delays for each channel pairing using the measured value for that channel pairing. These channel delays were all of the order of tens of picoseconds (Fig.7).

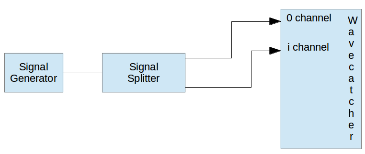

Figure 6: The scheme of the WaveCatcher channel calibration.

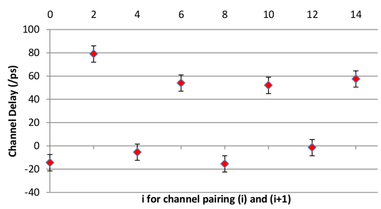

Figure 7: The dependence of time delays from the channel number [(i)-(i+1)].

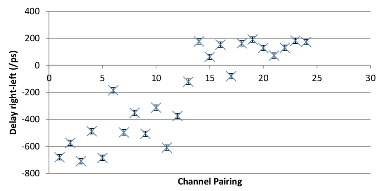

Figure 8: Delay associated with each NINO output channel pairing.

The WaveCatcher calibration method was extended to account for the delays introduced by all the electronics. Fig.8 displays the measured delay between the right and left electronic chains associated with each channel pairing of the NINO. The total accuracy for WaveCatcher and NINO is $\pm$ 20 ps for obtained values.

3.1.2 The dependence between time and signal width

Since the width of LVDS NINO output signal is proportional to the charge (amplitude) of the input signal to the NINO chip, there is a correlation between the width and the arrival time of the signal. This dependence was investigated with a dedicated test bench (Fig.9).

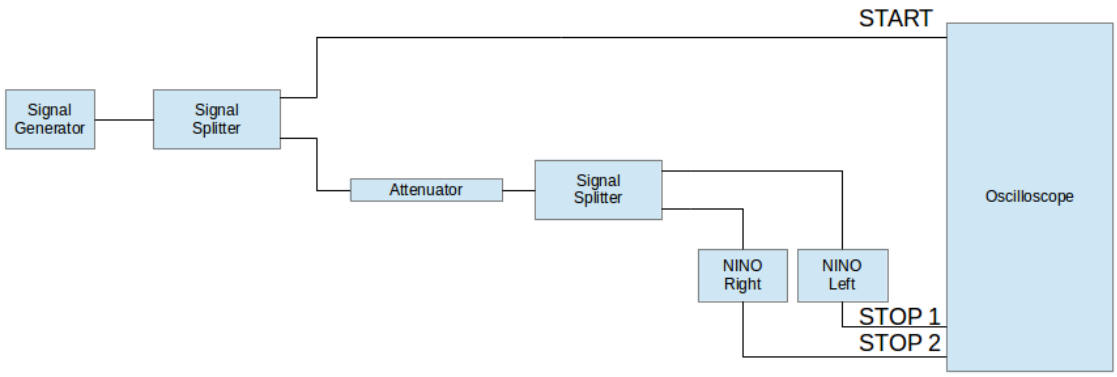

Figure 9: Scheme for the study of signal NINO motion.

Fig.10 and Fig.11 show the measurements taken from all channel pairings (R1-24 and L1-24) of each NINO board channels (upper and lower), where dt total (ps) is the total time-difference for a couple channels in picoseconds and Mean Width(ns) is the average of the signal width in nanoseconds.

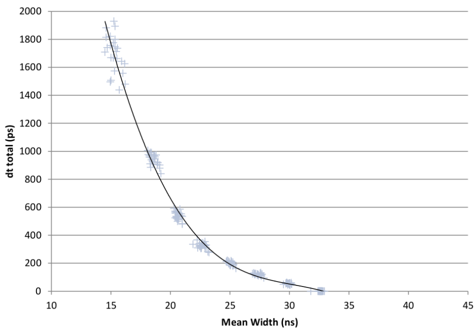

Figure 10: The variation of the time-difference with the mean width for the upper (left and right) NINO pair.

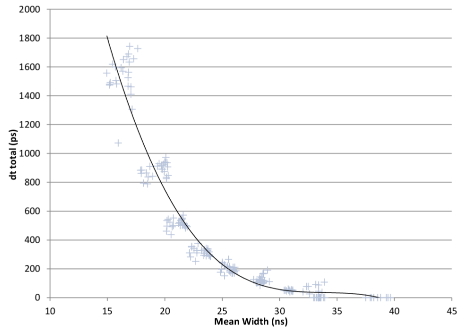

Figure 11: The variation of the time-difference with the mean signal width for the lower (left and right) NINO pair.

3.2 MRPC dark current as a function of voltage

Dark current in the MRPC is the relatively small electric current that flows through the chamber even when no muons are entering the device. It's from the background radiation, due to not ideally pure gas inside the chamber, electrical breakdown increasing with the voltage. It was decided to use the MRPC with a bias voltage around 16 kV where dark current is less than 1 μA (Fig.12), which is a good compromise between dark current and efficiency[6].

3.3 Measurement of the signal propagation speed along the strip

To measure the speed of the signal propagation along the strip (v), we use the setup shown on Fig.13: two plastic scintillators readout by PHILIPS Photomultipliers (XP2282/B SN:19239) and positioned one above the other are placed above one strip of the MRPC. When a muon passes through the scintillators and the corresponding strip, the electronic chain records signals from both ends of the strip. There

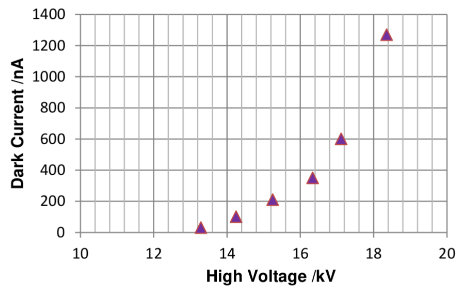

Figure 12: Dark current (nA) as a function of voltage (kV) for the upper MRPC with pure Freon.

have been several measurements at different points along the MRPC. Using the method described in the Subsection 2.4 of reconstruction of the hit and knowing the geometrical parameters of the experiment, the relationship between time difference of the signals at the ends of the strip and the location of the scintillators was constructed (Fig.14). The slope of the line determines the speed of the signal propagation along the strip. This value is 17.0 ± 0.4 cm/ns.

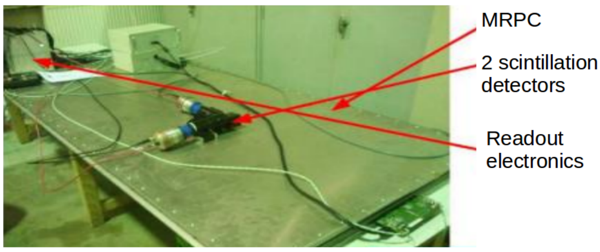

Figure 13: Setup used to determined v.

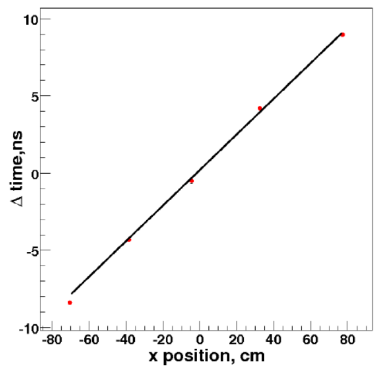

Figure 14: Difference between signal arrival time with variation of the position of muon incidence.

4 Acquisition and analysis of data

4.1 Map of MRPC registration efficiency

The errors of reconstructed data are due to different types of electronics false signals. To check the MRPC noise we turn on it without coincidences using scintillators to trigger the acquisition. As it turns out (Fig.15), the spectrum of the time difference has a periodic form, which is related to the fact that fishing thread that separates the glass plate inside the camera creates additional noise and its location is clearly visible in the reconstructed data (Fig.16).

4.2 Description of CORTO configuration in 2013

In order to decrease the noise ,three detectors were used to trigger CORTO: two short plastic scintillators ($5.0 \times 5.0 \times 1.5$ cm^3) and a long one ($3.0 \times 3.0 \times 60.0$ cm^3) with two photomultipliers at both ends.

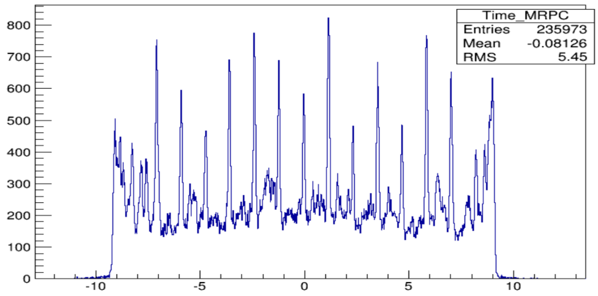

Figure 15: Distribution of the time difference from the left and right ends of the MRPC at startup without coincidences.

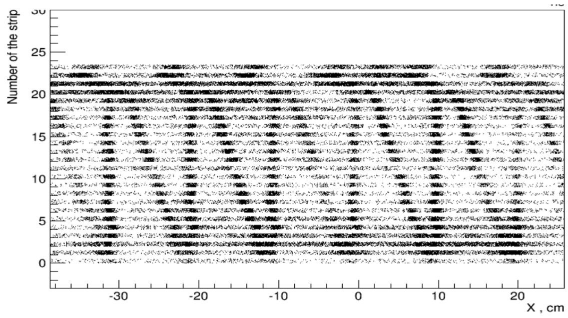

Figure 16: Generation of the noise by dividing thread between glass plates of the camera.

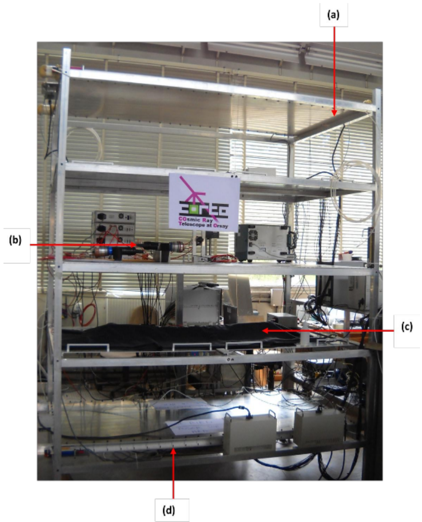

Figure 17: The scheme of the CORTO setup with scintillators.
(a) Top MRPC; (b) Two scintilation detectors; (c) "Long" scintillation detector; (d) Bottom MRPC

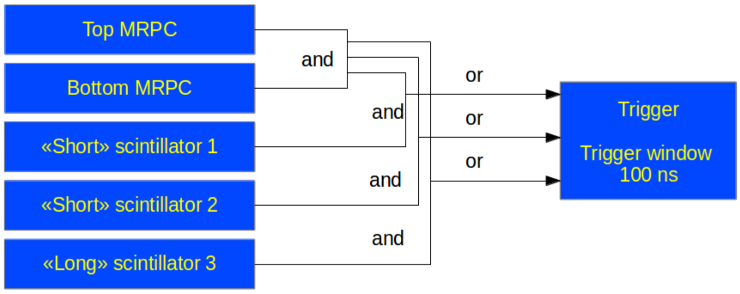

Figure 18: Coincidence circuit.

Knowing the speed of light in plastic scintillator (measured at LAL, $\sim$ 133 ps/cm) and measuring the time difference of signals on PMT, we can reconstruct the point of muon penetration.

Layout of the detectors is shown in Fig.17, all detectors (scintillators + PMTs and MRPCs) were included in the coincidence circuit (Fig.18) with a trigger window of 100 ns (time during which the system is waiting for signals from the detectors for one event).

To analyse the data from CORTO a C++ software using ROOT (CERN) was developed. Its main purpose is the reconstruction of events and the reducing of the size of data files for compact data storage on hard disk.

4.3 Muon impact point reconstruction

The Fig.19 and Fig.20 show the dependence between the reconstructed X coordinates using "Long" detector (y-axis) and using the procedure of the track reconstruction (x-axis) by CORTO. The linear dependence suggests that these two independent methods are consistent, even if there are noise samples

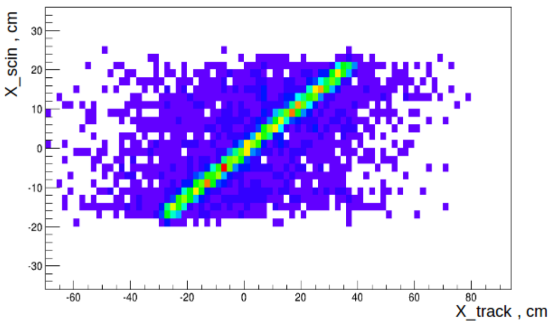

Figure 19: Dependence between reconstructed X-coordinates by "Long" detector and tracks from MRPC.

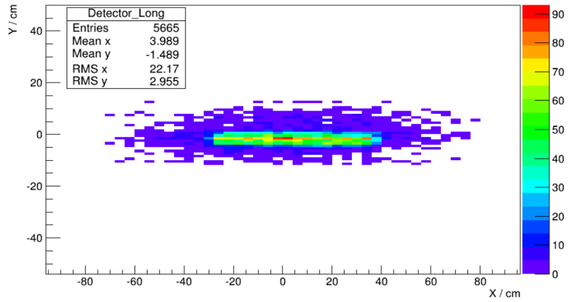

Figure 20: The two-dimensional histogram of the reconstructed position of "Long" detector.

that must be analysed and cut.

The Fig.21 (Fig.22) shows the distribution of the X (Y) coordinate for "Long" scintillator as a result of the events reconstruction. For the Y coordinate, the sigma of the distribution is 1.69 cm (FWHM = 3.98 cm), for X coordinate: sigma is 3.36 cm (FWHM = 75 cm). For "Short" detector, the distribution has a Gaussian form with a sigma of 1.814 cm (FWHM of 4.27 cm). Similarly, for Y coordinates sigma is 2.13 cm (FWHM 5.02 cm). If we recall that the size of scintillators is 5 cm by 5 cm on X and Y, it can be concluded that the tracks are correctly reconstructed.

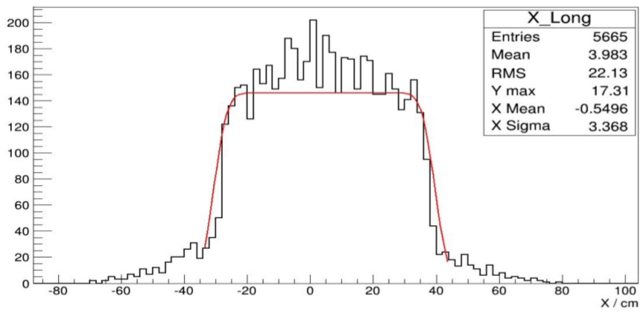

Figure 21: Distribution of X coordinate for "Long" scintillator.

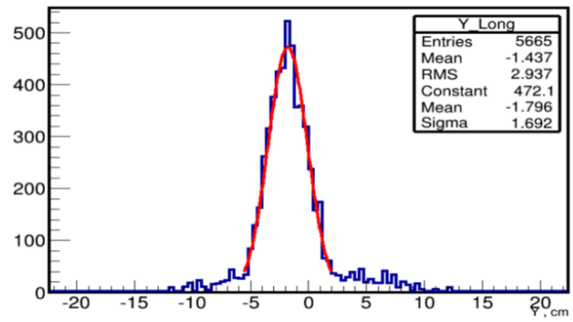

Figure 22: Distribution of Y coordinate for "Long" scintillator.

A simulation of the CORTO and detector setup using the same software package ROOT (CERN) was performed, the particles were generated with a given angular distribution ($cos^{1.85}(\theta)$)[1]. The Fig.23 and Fig.24 show the comparison of simulation and experimental data for distribution of X and Y coordinates of the "Long" detector. Those two results (simulation and experimental) are consistent.

5 Conclusions

The preliminary test of the COsmic Ray Telescope at Orsay gives encouraging results: a time resolution of 250 ps (for a bias voltage of 16 kV), a spatial resolution along the X direction of 1.8 cm and along the Y direction of 2.1 cm. So it's possible to use CORTO for testing different types of detectors using cosmic rays.

Improvement version of CORTO with better characteristics (100 ps of limiting resolution, around 1 cm of spatial resolution) is planned in 2014. Once finalized, CORTO will be opened to other laboratories

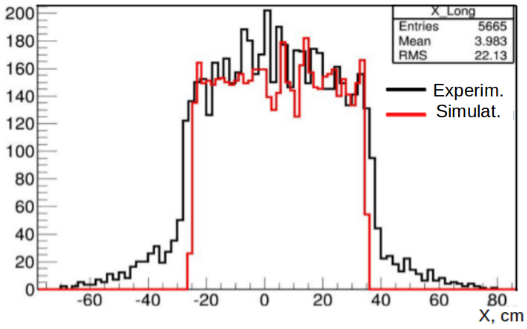

Figure 23: Comparison of experimental and simulated data for the X coordinate of the "Long" detector.

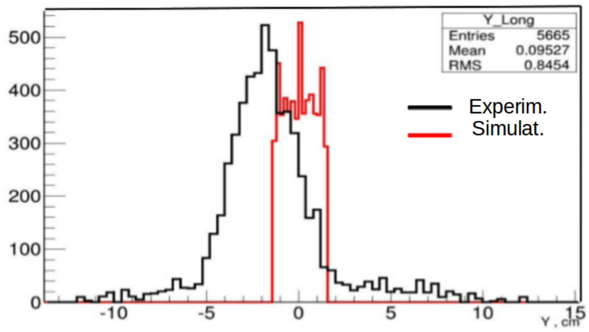

Figure 24: Comparison of experimental and simulated data for the Y coordinate of the "Long" detector.

and used by students during their Master as a testing platform.

6 List of references.

1. Cosmic Rays at Earth (Researcher's Reference Manual and Data Book) - Peter K.F.Greider - Institute of Physics,University of Bern[Bern 2001,Switzerland].

2. S. An et al., Multigap resistive plate chambers for EAS study in the EEE Project, Nuclear Instruments and Methods in Physics Research Section A: Accelerators, Spectrometers, Detectors and Associated Equipment, Volume 581, Issues 1–2, 21 October 2007, Pages 209-212, ISSN 0168-9002, 10.1016/j.nima.2007.07.079.
(http://www.sciencedirect.com/science/article/pii/S0168900207015458)

3. D. Breton, E. Delagnes, J. Maalmi, Using ultra fast analog memories for fast photodetector readout, Nuclear Instruments and Methods in Physics Research Section A: Accelerators, Spectrometers, Detectors and Associated Equipment, Volume 695, 11 December 2012, Pages 61-67, ISSN 0168-9002, 10.1016/j.nima.2011.12.007.
(http://www.sciencedirect.com/science/article/pii/S0168900211021668)

4. NINO: an ultra-fast and low-power front-end amplifier/discriminator ASIC designed for the multigap resistive plate chamber.

5. F. Anghinolfi et al., "NINO: an ultrafast low-power front-end amplifier discriminator for the time-of-flight detector in the ALICE experiment," Nuclear Science, IEEE Transactions on , vol.51, no.5, pp.1974,1978, Oct. 2004 doi: 10.1109/TNS.2004.836048
F. Anghinolfi, P. Jarron, A.N. Martemiyanov, E.Usenko, H. Wenninger,M.C.S. Williams,A.Zichichi

6. EEE Project: Report on scientific activity.
Frolov Vladimir

7. Nuclear Instruments and Methods in Physics Research A: Performance of a six gap MRPC built for large area coverage.
M. Abbrescia, A. Alici , S. An, A. Badala, Y.W. Baek R. Baldini Ferroli, G. Bencivenni, F. Blanco,E. Bressan, A. Chiavassa , C. Chirii,j, C. Cicalo, L. Cifarelli, A. De Caro, D. De Gruttola et al.

8. CORTO: Year in Europe Project report.
   Edward William Karl Bals, Imperial College, London.
9. TWEPP-09: Picosecond time measurement using ultra fast analog memory.
   D.Breton, E.Delagnes, J.Maalmi
10. Sazonov A.B. // Lectures on nuclear physics - Mendeleev Russian University of Chemical Technology.